Characterization of the structural-electronic effects in $LaFe_{1-x}Ga_xO_3$ and $LaMn_{1-x}Ga_xO_3$ by oxygen K-edge x-ray absorption using a multiple scattering analysis

S Lafuerza[1], G Subías[1,4], J García[1], S Di Matteo[2], J Blasco[1], V Cuartero[1], and C R Natoli[1,3]

[1] Instituto de Ciencia de Materiales de Aragón (ICMA), CSIC-Universidad de Zaragoza, Departamento de Física de la Materia Condensada, Pedro Cerbuna 12, 50009 Zaragoza, Spain

[2] Inst Phys Rennes, Univ Rennes 1, UMR CNRS-UR1 6251, F-35042 Rennes, France

[3] Laboratori Nazionali di Frascati INFN, C.P. 13, I-00044 Frascati Roma, Italy

E-mail: gloria@unizar.es

Abstract

We report on experimental oxygen K-edge x-ray absorption near-edge structure (XANES) spectra of the $LaFe_{1-x}Ga_xO_3$ and $LaMn_{1-x}Ga_xO_3$ series. The transition-metal substitution by the 3d full shell Ga atom is mainly reflected in a systematic decrease of the pre-edge structures in the XANES spectra of the two series. This result shows that the associated states originate from the hybridization of oxygen 2p and unoccupied Fe (or Mn) 3d states. We have analyzed the experimental results in terms of detailed calculations based on multiple-scattering theory. In order to relate the pre-edge features to the corresponding atomic arrangements and electronic characters, we performed simulations with variable cluster size and composition around the absorber oxygen in the $LaFeO_3$ and $LaMnO_3$ crystal structures. We find that the low-energy pre-peak is correctly reproduced if just the absorbing oxygen and the two nearest neighbours Fe (or Mn) ions are considered in the cluster. Conversely, higher energy pre-peaks only arise when the full oxygen-coordination geometry around the two metal sites is taken into account. The coupled electronic and structural origin of the pre-peaks successfully explains the difference observed in the pre-edge structures between the XANES spectra of $LaFeO_3$ and $LaMnO_3$.

PACS: 61.05.cj, 61.05.jd, 75.47.Lx

Submitted to Journal of Physics: Condensed Matter

[4] Author to whom any correspondence should be addressed.

1. Introduction

Properties of materials are determined by their geometrical and electronic structure. Under this assumption, several electron spectroscopies have long been used to resolve the electronic structure of materials with the aim to study its correlation with the macroscopic properties. Given the profuse and rich variety of phenomena they exhibit, transition metal oxides and, in particular, the perovskites with general formula ABO_3 containing a rare-earth metal on A sites and a 3d-transition-metal on B sites, are of great importance for both applied and fundamental researches. The electronic structure of these materials has been intensively studied especially after the discovery of high temperature superconductivity, of colossal magnetoresistance, and of multiferroicity, as reviewed, e.g., in [1], [2], [3], respectively. One important aspect in order to understand their phenomenology resides in the bonding of oxygens and 3d-transition-metals. X-ray absorption near edge structure (XANES) spectroscopy at the oxygen K-edge is the appropriate technique to investigate this bonding, since information on the electronic states projected on the oxygen atom site is obtained by this technique. The O K-edge involves transitions of an electron from the oxygen 1s core level to unoccupied final states of p symmetry as required by dipole selection rules. The oxygen K-edge XANES spectra are usually interpreted by either band structure (BS) or multiple scattering (MS) theoretical calculations. In the BS approaches [4] the spectral features are explained by comparison with the atomic and symmetry projected density of states (DOS), which is calculated using the density functional theory [5]. These methods, typically developed in reciprocal space, use the three-dimensional periodicity of the material and thus are restricted to ordered systems. On the other hand, the MS [6, 7] calculations use a cluster model and are carried out in real space. Within this framework, the x-ray absorption cross section is computed using the cluster Green's function. Generally, relatively small clusters extending up to ~ 6 Å from the photo-absorbing atom are enough to reproduce the experimental data. Both methods calculate the site and symmetry projected DOS and in the case of ordered systems they are equivalent, if due account is taken of the finite lifetime of the excited final states. However the MS approach is not restricted to these latter systems, since the projected DOS is obtained in a physically intuitive way by calculating the imaginary part of the scattering amplitude of the excited photo-electron for all the closed paths in the system beginning and ending at the photo-absorber. This procedure does not require periodicity and in addition the contribution of each individual path to the local DOS can be identified.

In many 3d-transition-metal oxides the transition metal is octahedrally coordinated with ligand oxygens. For perfect octahedral symmetry, the 5-fold degenerate 3d band of the transition metal splits into the three lower energy orbitals t_{2g} and the two higher energy orbitals e_g. The e_g orbitals lie along the bonding axes between the transition metal and the oxygen and thus they experience a stronger repulsion being higher in energy than the t_{2g} ones, which point away from the oxygen atoms. A common feature in the O K-edge XANES spectra of oxides

containing a 3d-transition-metal in octahedral symmetry is the presence of a well differentiated double structure in the pre-edge region [8-12]. As interpreted by BS approaches, this spectral feature relates to the hybridization of the O 2p states with the transition metal 3d band. The total DOS is separated into the oxygen and transition metal contributions and the two pre-edge structures are simply ascribed to the t_{2g} and e_g band-like states split by the ligand field [13-15]. The so-called pre-peaks in the O K-edge XANES were first attributed to the t_{2g} and e_g states by de Groot *et al* (1989) [8], arguing a correspondence between the energy peak separation and the ligand-field-splitting obtained from optical data for octahedrally hydrated transition metal ions. However, serious discrepancies come up following this assumption as the experimental t_{2g}:e_g intensity ratios in the XANES do not agree either with electron counting or with orbital hybridization ideas.

In this work we intend to provide a deep insight into the character of the pre-peaks by means of a combined experimental and theoretical approach.

The materials chosen for this purpose are the archetypal perovskites $LaFeO_3$ and $LaMnO_3$. In the first, the Fe atom is near octahedrally coordinated by oxygen atoms, whereas in $LaMnO_3$ there is a tetragonal distortion of the MnO_6 octahedron due to the Jahn-Teller effect that further splits the t_{2g} and e_g levels. Since both compounds admit the transition metal substitution by the 3d full band Ga atom, the $LaB_{1-x}Ga_xO_3$ (B = Fe, Mn) series are ideal candidates to investigate the relevance of the solid-state effects in the O K-edge XANES spectra as well as the electronic character of the pre-edge structures. In the $LaBO_3$ perovskite-like compounds the BO_6 octahedra share O^{2-} ligands, so the B substitution by Ga causes a mismatch in the lattice which in turn modifies the strong O 2p – B 3d hybridization. $LaFeO_3$ and $LaMnO_3$ are antiferromagnetic insulators with the Néel temperature T_N of ≈ 740 and 140 K respectively. Ga^{3+} is homovalent with both Fe^{3+} in $LaFeO_3$ and Mn^{3+} in $LaMnO_3$, and the $LaGaO_3$ perovskite is a typical insulator because of the $3d^{10}$ electronic configuration of Ga^{3+}. Fe substitution by Ga in $LaFeO_3$ reduces the antiferromagnetic interaction, lowering T_N to ≈ 215 K for x = 0.5 [16], whereas it induces a change to a canted ferrimagnet for $x < 0.5$ and to a ferromagnet for $x \geq 0.5$ in $LaMnO_3$ [17]. In both series the main structural change produced by Ga dilution is to progressively eliminate the long-range ordered transition metal in the $LaFeO_3$ and $LaMnO_3$ lattices giving way to isolated Fe^{3+} and Mn^{3+} ions respectively. The FeO_6 octahedra remain regular in the whole range of composition, while the tetragonal distortion of the MnO_6 octahedra in $LaMnO_3$ decreases continuously as Ga replaces Mn, becoming almost symmetric octahedra for $x \geq 0.6$ [17,18].

We have opted for the MS formalism as it is particularly useful for the study of the O K-edge XANES spectra in the $LaFe_{1-x}Ga_xO_3$ and $LaMn_{1-x}Ga_xO_3$ homovalent-substituted systems. Calculations based on the MS theory have shown to satisfactorily reproduce the experimental O K-edge XANES spectra of several transition metal oxides [19-21]. One advantage over the BS methods is that by comparison of MS calculations performed for increasing cluster sizes,

relating the different atoms around the absorber to the spectral features comes naturally. Besides, the analysis in polarization of the theoretical calculations allows obtaining the type of symmetry in selected bonding directions. Finally and of major convenience for the series under study here, the effect of changing the chemical species of only certain atoms within the cluster can be monitored.

The outline of the paper is organized as follows. Experimental and calculation details are presented in section 2. Next section 3 is devoted to the description of the experimental results with emphasis on the evolution of the pre-edge structures with gallium content. The section 4 covers the MS theoretical analysis of the O K-edge XANES spectra. Lastly, in section 5 we discuss the characteristics of the unoccupied electronic states associated to the pre-edge structures and we conclude with an alternative description for them.

2. Experimental and calculation details

Polycrystalline $LaFe_{1-x}Ga_xO_3$ (x = 0, 1/3, 0.5, 2/3, 0.8, 0.9) samples were prepared following a conventional ceramic procedure. At a first stage, stoichiometric amounts of La_2O_3, Fe_2O_3, and Ga_2O_3 were mixed, milled, and fired at 1000 ºC for 12 h in air. Then, the resulting powders were milled, pressed into pellets and sintered at 1200 ºC for 24 h in air. Finally, the latter procedure was repeated by sintering the repressed pellets at 1400 ºC for ~ 48 h. X-ray powder diffraction analysis of all the samples was performed in a Rigaku DMAX 2000 diffractometer with a rotating anode and selecting the Cu K_α radiation. Every sample ($0 \leq x \leq 0.9$) was confirmed to be single phase in an orthorhombic structure with space group *Pnma*. Introduction of Ga in the $LaFeO_3$ lattice induces least structural modifications, the only significant change being a slight contraction of the unit cell with increasing Ga content x (from 243.468 $Å^3$ for the x = 0 sample to 236.965 $Å^3$ for the x = 0.9 sample). The Ga atoms occupy the Fe sites and the Fe(Ga)-O distances indicate the maintenance of regular oxygen octahedra around Fe(Ga) for the whole range $0 \leq x \leq 0.9$. Powder $LaMn_{1-x}Ga_xO_3$ (x = 0, 0.1, 0.2, 0.3, 0.5, 2/3, 0.8, 0.9) samples were synthesized also by means of a conventional ceramic procedure and preparation details as well as information on how the structure is affected by Ga dilution can be found in [17,18].

The O K-edge XANES measurements were carried out on the BEAR beamline of the ELETTRA synchrotron in Trieste, Italy. All the spectra were measured in the total electron yield (TEY) mode at room temperature on sintered pellets. The vacuum chamber base pressure was below 1×10^{-10} Torr. The energy resolution was 200 meV for a typical photon flux on the sample of the order of 10^{10} ph/s [22]. The experimental XANES spectra have been normalized to 1 in the high energy part after a linear background subtraction so as to be compared.

Theoretical calculations were performed using the FDMNES code [23] in the MS real-space approach, within the muffin-tin (MT) approximation for the potential. Overlapped atomic densities resulting from a Hartree-Fock-Dirac program were used to calculate the charge density of the cluster, allowing a 10 % overlap between the MT spheres. The exchange-correlation part

of the potential was taken as the real Hedin, Lundqvist and Von Barth potential. The spectra were convoluted using a lorentzian function with a constant broadening to simulate the core level width, which was automatically determined by the program, and an additional energy dependent broadening to account for the final state width using an arctangent formula [23b]. This latter is intended to simulate inelastic extrinsic losses due to plasmon and particle-hole excitations into the system. The real orthorhombic crystal structures of $LaFeO_3$ [24] and $LaMnO_3$ [25] were employed to obtain the atomic positions.

3. Experimental results

The normalized O K-edge XANES spectra of $LaFeO_3$ and $LaMnO_3$ measured at room temperature are shown in figure 1. These spectra are similar to previously reported ones [21, 26]. Three different regions can be identified in the spectra. The first one, extending from 528 to 533 eV and commonly referred to as the pre-edge region, is described as oxygen 2p states hybridized with the transition metal 3d ones [8]. The next region covers the 533 – 538 eV range and it is explained as the mixing between oxygen 2p states with La atoms 5d states [10,21]. The region above 538 eV is attributed to mixing with higher energy states of the transition metal and La atoms [10,21].

The two spectra exhibit a marked difference in the pre-edge region. Whereas two well defined sharp pre-peaks appear for $LaFeO_3$, a doublet is hardly resolved in the $LaMnO_3$ spectrum within the experimental resolution. For $LaFeO_3$ the energy separation between the two pre-peaks is about 1.4 eV, similar to the separation found in hematite (α-Fe_2O_3) [19]. For $LaMnO_3$, we estimate that the width of the doublet in the XANES spectrum (see vertical lines in figure 1) is approximately 0.8 eV. This energy separation is usually correlated to the crystal field splitting [8,10]. We will discuss this difference later in the view of the results from MS calculations. Moreover, a chemical shift of the pre-edge structure to lower energies is observed in the $LaMnO_3$ spectrum with respect to the position of the pre-peaks in the $LaFeO_3$ one. The formal valence states for the transition metal ions in the two compounds are Mn^{3+} ($3d^4$) and Fe^{3+} ($3d^5$). It hence follows that the oxygen K-edge spectra of $LaBO_3$ (B = Fe, Mn) shift to lower energy with the reduction of d electrons, which is in agreement with results reported in related transition-metal perovskites [12,26,27].

Figure 2 presents the normalized O K-edge XANES spectra of $LaFe_{1-x}Ga_xO_3$ (x = 0, 1/3, 0.5, 2/3, 0.8, 0.9) and $LaMn_{1-x}Ga_xO_3$ (x = 0, 0.1, 0.2, 0.3, 0.5, 2/3, 0.8, 0.9) series measured at room temperature. Two important changes with Ga doping can be appreciated in the spectra of both series. First of all, in the pre-edge region, there is a systematic intensity decrease of the pre-peaks, labelled as A and B, along with increasing Ga content (x). Secondly, the broad feature centered about 535 eV, denoted as C, tends to grow in intensity as x increases. In the high-energy region above 538 eV, the spectral shape of the doped samples does not change notably, for either $LaFe_{1-x}Ga_xO_3$ or $LaMn_{1-x}Ga_xO_3$.

The Fe^{3+} ($3d^5$) and Mn^{3+} ($3d^4$) substitution by the fully occupied Ga^{3+} ($3d^{10}$) reduces the number of accessible empty d levels avoiding the mixing with the O 2p states. Therefore, the effect of diminishing the pre-peaks as Ga replaces Fe and Mn provides direct experimental evidence that the pre-edge structure in the O K-edge XANES of transition metal oxides originates from O 2p states hybridized with the unoccupied metal 3d states [8]. In order to quantify this effect, the area of the well separated pre-peaks A and B in the spectra of $LaFe_{1-x}Ga_xO_3$ has been estimated. The A and B peaks have been fitted to a lorentzian function each after a baseline subtraction and then the integrated area of the fitted curves has been calculated. In figure 3 is shown the normalized integrated area of the A and B peaks for the $LaFe_{1-x}Ga_xO_3$ series as a function of Ga content (x). It can be observed that the intensity decrease of the A and B peaks scales almost linearly with increasing x, the peak B showing a slightly sharper drop. This means that while peak A is proportional to the transition metal content and its origin is the O 2p – Fe 3d mixing exclusively, in peak B some other effects, probably long-range, should be considered. In the $LaMn_{1-x}Ga_xO_3$ series the strong overlap of the two pre-peaks did not allow such a quantitative calculation, and yet, qualitatively, they appear to follow a similar tendency.

The feature C tends to increase in intensity with Ga doping, and it seems that some spectral weight is transferred from the pre-peaks to this structure. This means an enhancement of the hybridization between O 2p and La 5d states as a side effect of the reduction in the O 2p – B 3d (B = Fe, Mn) hybridization.

4. Multiple-scattering analysis

With the aim to characterize the spectral features in the experimental O K-edge XANES of the $LaFeO_3$ and $LaMnO_3$ compounds and clarify its evolution on substituting Ga, we have carried out a thorough theoretical analysis in the MS approach. In order to do that, several calculations were performed by using clusters of atoms around the absorber oxygen with variable size and composition.

For the $LaFeO_3$ compound, we used the orthorhombic perovskite unit cell with lattice constants a = 5.5595 Å, b = 7.8498 Å, and c = 5.5509 Å (*Pnma* space group) [24]. The Fe and La atoms are in the 4b and 4c crystallographic sites respectively and for the O atoms there are two non-equivalent sites: 4c (O1) and 8d (O2). Calculations separately for each oxygen site show qualitatively the same results and for simplicity we only discuss the simulations of the 4c site absorber oxygen contribution.

For $LaMnO_3$, the lattice parameters of the orthorhombic cell are a = 5.5367 Å, b = 5.7473 Å, and c = 7.6929 Å (*Pbnm* space group) [25]. Similarly to the $LaFeO_3$ compound, the Mn and La atoms are in the 4b and 4c crystallographic sites and the O atoms are in the two different sites 4c (O1) and 8d (O2). However, in the case of $LaMnO_3$ the calculations yield very different results for each of the oxygen sites and for that reason these calculations are discussed in detail for both the O1 and O2 site atoms.

Our strategy was twofold:

i) We calculated spectra for increasing cluster radius in order to relate their most significant features to the different atoms (scattering paths) around the absorber oxygen. Also a polarization analysis was performed here.

ii) We calculated spectra for different Ga-atoms substitutions to simulate the effect of gallium doping in the theoretical spectra.

For the sake of comparison, the theoretical values of energies in the calculations have been aligned to the experimental energy scale so that the first pre-peak coincides.

a. $LaFeO_3$

i) Increasing cluster radius

Several clusters around the central O1 (4c site) atom were selected for the simulations by looking at the distribution of bond distances in $LaFeO_3$. In figure 4 we report the significant results which correspond to calculations within the cluster radii of 2.0 Å (3 atoms), 3.2 Å (15 atoms), 3.5 Å (17 atoms), and 4.0 Å (19 atoms). The radial distances distribution around O1 up to 4 Å is provided in table 1 so as to identify the atoms included in each of the cluster sizes.

For the 2.0 Å cluster calculation which solely includes the first coordination shell, only one resonance centered at about 530.5 eV arises that we have identified as the pre-peak A of the experimental spectrum. The first shell consists of the two Fe nearest neighbours (NN) surrounding the central oxygen ($O1_{abs}$) atom, and accordingly pre-peak A represents transitions to 3d states of the two Fe NN hybridized with O 2p states. When adding the next shell of neighbouring atoms, which extends up to 3.2 Å and contains 4 La atoms and 8 O2 atoms (see table 1), the structure of the spectrum becomes more similar to the experimental one: besides the well separated low-energy pre-peak, two bands at energies about 536 and 542 eV come out. The band at ~ 536 eV is a feature corresponding to structure C in the experimental spectrum. If either the La or the O2 atoms in the second shell are removed in the calculation, this band does not form, indicating that it stems from the hybridization between O 2p states and La 5d states. A second resonance at ~ 532.5 eV is obtained when the cluster radius reaches 4 Å (note that it does not appear in the calculation up to 3.5 Å) that we characterize as pre-peak B. The pre-peak B arises once the two O1* atoms are included, which in turn means the completion of the oxygen octahedral coordinations of the two Fe NN. A picture of the 4.0 Å cluster around $O1_{abs}$ is illustrated in figure 5. In order to gain a deeper understanding about the origin of peak B, we have considered how the calculation is affected when the oxygen octahedra surrounding the two Fe atoms are broken. For that, we have carried out a simplified 4.0 Å radius cluster calculation where the 8 O2 atoms forming the octahedra around the two Fe NN (see figure 5) have been removed. In the simplified calculation there is no trace of the high-energy resonance at ~ 532.5 eV (the low-energy one is still seen). The latter result demonstrates the need of having the two Fe NN coordinated by their complete oxygen octahedra for the formation of this state. This

finding confirms that peak B is strongly dependent on the geometry of the neighbouring Fe atoms.

We have also studied the polarization dependence of the two pre-peaks A and B within the 4.0 Å radius cluster. The polarized results were calculated for only one of the four equivalent O1 atoms in the unit cell so as to characterize the type of symmetry in the bonding associated to each peak. The polarized XANES spectra with the x-rays polarization vector *E* parallel to the [100], [010], and [001] crystallographic directions are shown in figure 6. The [010] direction corresponds closely to the direction along the O1*-Fe-$O1_{abs}$-Fe-O1* path, and the [100] and [001] are orthogonal to it. We observe that peak A at ~ 530.5 eV is absent along [010], while it appears with the same intensity in both the [100] and [001] directions. The peak B at ~ 532.5 eV shows the opposite behaviour, being observed only when the polarization vector lies in the [010] direction. In terms of a molecular-orbital picture, the low-energy resonance would correspond to the formation of a π-antibonding (π*) O-Fe bond whereas the high-energy one would be related to a σ-antibonding (σ*) O-Fe bond.

Finally, in figure 7 we also present the MS simulation summed over the two oxygen crystallographic sites 4c (O1) and 8d (O2) using a cluster of 9.1 Å (~ 260 atoms), where the overall evolution of the spectral features has reached convergence. The agreement between the MS theoretical calculation and the experimental O K-edge XANES of $LaFeO_3$ is quite good, except for an overall energy-scale factor indicating the need for a more-attractive potential. It can be observed that as we increase the cluster size, the intensity of the pre-peaks decreases with respect to the other spectral features, specially the one of pre-peak B. This fact indicates that the high-energy pre-peak is more sensitive to long-range order than the low-energy one. This means that although the associated states are mainly atomic, i.e. a small cluster is enough to reproduce them; they are also influenced by more distant atoms beyond 4 Å.

ii) Ga atoms substitutions

The next step is to study how the theoretical spectra are affected by gallium substitutions in the cluster. Again, we have focused on the 4.0 Å radius cluster calculation for $LaFeO_3$ as it is the smallest cluster size for which the main experimental spectral features are reproduced. We recall that only the 2 Fe NN atoms of the O1 absorber oxygen are contained inside this cluster (see table 1). These two Fe atoms are at the same distance from the O1 atom and therefore there are two possibilities: 1 Fe NN substituted by 1 Ga atom, and 2 Fe NN substituted by 2 Ga atoms; that have been considered. The 4.0 Å radius cluster calculations for $LaFeO_3$ with the mentioned Ga substitutions are reported in figure 8. They show the same general behaviour as the experimental XANES of the $LaFe_{1-x}Ga_xO_3$ series, indicating that the two A and B pre-peaks appear if at least one of the two NN is an iron atom. When 1 Ga atom substitutes 1 Fe NN the two pre-peaks weaken abruptly to nearly half their intensity. For 2 Ga atoms as NN both are absent. These results corroborate that oxygen needs empty 3d states in the NN for the appearance of the two pre-peaks (the higher energy one with the additional condition of the NN

being surrounded by complete oxygen octahedra). Furthermore, the decrease of the pre-peaks intensity is coupled to the increase of the broad peak at ~ 536 eV as seen experimentally.

b. $LaMnO_3$

i) Increasing cluster radius

Based on the bond distances distribution for the O1 (4c site) and O2 (8d site) oxygen atoms in $LaMnO_3$, different cluster radii were selected for each oxygen site to perform the calculations. For the O1 atom, the relevant simulations correspond to the cluster radii of 2.0 Å (3 atoms), 3.3 Å (15 atoms), 3.5 Å (17 atoms), and 4.0 Å (19 atoms). The cluster around the O2 atom is much more asymmetric compared to that of O1 and the significant radii are 2.2 Å (3 atoms), 3.4 Å (17 atoms), 3.9 Å (18 atoms), and 4.4 Å (26 atoms). The radial distances distribution around O1 and O2 up to 4.0 and 4.4 Å respectively, are given in table 2. In figure 9 are shown the O K-edge XANES calculations individually for both the O1 (upper panel) and O2 (lower panel) atoms in $LaMnO_3$ for growing cluster radii.

Calculations for the O1 atom resemble those already discussed for the $LaFeO_3$ compound. A low-energy pre-peak located at 530 eV appears for the 2.0 Å cluster in which only the two Mn NN of the first coordination shell are accounted for, thus involving transitions to empty 3d Mn states hybridized with O 2p states. For a 3.3 Å cluster, that also contains 4 La and 8 O2 neighbouring atoms, two additional bands at higher energy show up. Finally, in the 4.0 Å cluster radius the two Mn NN are coordinated by 6 oxygen atoms each and a higher energy pre-peak around 532.5 eV becomes visible. We note that the energy separation between these two pre-peaks is about 0.5 eV larger than in the $LaFeO_3$ case. We have checked the effect of changing the two Mn NN by Fe atoms in the cluster around O1 maintaining the distances yielded by the $LaMnO_3$ crystal structure. As a consequence of this substitution, only a global energy shift of the pre-peaks takes place. This result implies that while the energy separation of the pre-peaks is determined by the surrounding crystal structure, their energy position mainly depends on the 3d electronic configuration.

The geometry around the O2 atom is markedly different. The first coordination shell is formed by two Mn atoms at the very different radial distances of 1.906 and 2.180 Å (see table 2). Similarly to the previous cases, a low-energy resonance at 530 eV is observed in the calculation within a cluster of 2.2 Å. Once again, two bands form at higher energies when the following shell of La and O atoms is included, this being observed in the 3.4 Å cluster simulation. In what follows, the key is in the O2 atoms located at 3.811 and 4.360 Å (denoted as O2* and O2** respectively) from the absorber O2 ($O2_{abs}$). A picture of the 4.4 Å cluster around $O2_{abs}$ is shown in figure 10 to understand the role of the O2* and O2** atoms. So far, when the cluster size was such that the oxygen octahedra of the two NN transition metals were fully completed, an additional resonance was observed in the calculation at the right side of the low-energy one. In this case, the oxygen octahedron of the near Mn NN (at 1.906 Å) from $O2_{abs}$ is

completed when the O2* at 3.811 Å is included in the 4.0 Å cluster; while the octahedron of the far Mn NN (at 2.180 Å) does not complete until the O2** at 4.360 Å is accounted for in the 4.4 Å cluster calculation. Therefore, as can be noted in figure 9, for the O2 absorber oxygen atom in the $LaMnO_3$ compound there are two different resonances depending on whether the oxygen octahedral environment is provided either for the near or the far Mn NN. A pre-peak located at 532.5 eV appears when the octahedron of the near Mn is completed, and another one shows at 531 eV when the same occurs for the far Mn. Additional calculations have been performed with removals of some oxygen atoms forming the octahedra of each of the two Mn NN. The pre-peak at 532.5 eV disappears when the octahedron of the near Mn breaks up, and the one at 531 eV vanishes if so does the octahedron of the far Mn. Moreover, if the two Mn NN are replaced by 2 Fe atoms in the distorted 4.4 Å cluster around O2 as checked in the calculation for O1, the three pre-peaks move together in energy. This indicates that the structure dictates the number of resonances, as well as the energy separation between them. Besides, it is noteworthy that the higher energy pre-peaks present in the calculation for O2 are considerably lower in intensity than the high-energy pre-peak for the O1 calculation. The distorted structure around O2 seems to minimize the intensity of these resonances.

In figure 11 is displayed a calculation within a cluster of 9.1 Å (~ 250 atoms) summed over the O1 and O2 atoms to be compared with the experimental spectrum of $LaMnO_3$. As for the $LaFeO_3$ system, the converged MS simulation adequately agrees with the experimental O K-edge XANES. It can be seen that in the 9.1 Å cluster radius calculation the higher energy pre-peak located at 532.5 eV mixes with the broad band centered at 535 eV, this resembling more the experimental spectral shape. Again, the pre-edge features are very influenced by long-range order, mainly the higher energy ones.

ii) Ga atoms substitutions

Also for the $LaMnO_3$ compound we have examined the effect of substituting the two NN Mn atoms by Ga atoms in the calculations. For the O1 atom the two Mn NN are at the same radial distance and therefore only the two possibilities 1 Mn NN substituted by 1 Ga atom, and 2 Mn NN substituted by 2 Ga atoms; have been considered. In the O2 atom case, given that the 2 Mn NN are at different distances, in the calculation with substitution of only 1 Mn NN, we have made a distinction between the replacement of the near and far Mn. For O1, as it is shown in figure 12 (upper panel), the two pre-peaks disappear with Ga substitution of the two Mn NN atoms. This definitely confirms our previous statement, that is empty 3d states are needed for the formation of these states. The partial substitution of the Mn NN induces, as in $LaFeO_3$, a strong decrease of the pre-peaks intensity. Moreover, the high-energy peak at 532.5 eV is now mixed with the band at 535 eV. The global effect originated by the substitution of the two Mn NN atoms around the O2 atom is similar to the O1 atom since the pre-peaks, three in this case, also vanish when the two Mn atoms are substituted (see lower panel in figure 12). Alternatively, the substitution of only one Mn atom produces different effects in the XANES spectra

depending on which of the two Mn is substituted. While the substitution of the near Mn NN makes only the pre-peak at 532.5 eV disappear, the one at 531 eV vanishes when the far Mn NN is replaced.

Since the gallium dilution in $LaMnO_3$ induces structural changes in the lattice, the latter study can only be used as a theoretical characterization of the spectral features but not as the simulation of the behaviour observed in the experimental XANES of $LaMn_{1-x}Ga_xO_3$ upon Ga substitution. The replacement of Mn by Ga induces a decrease of the orthorhombic distortion of the cell in $LaMnO_3$, being the tetragonal distorted Mn octahedra practically regular for gallium concentration $x \geq 0.6$ [17,18]. In order to simulate the experimental behaviour more realistically, we have also checked the effects of Ga substitutions in equivalent calculations performed for the crystal structure of the highly diluted $LaMn_{0.1}Ga_{0.9}O_3$ sample [17]. The major difference is in the simulations for the O2 atom, whose environment is much more symmetric with the two Mn NN at the radial distances of 1.973 and 1.977 Å. Apart from the low-energy pre-peak at 530 eV arising when simply considering the two Mn NN in the cluster, only one more appears at the higher energy of 532 eV when including the oxygen atoms forming their oxygen octahedra. The latter is notably larger in intensity than the two high-energy pre-peaks obtained in the analogous simulation around O2 for the distorted $LaMnO_3$ crystal structure. Both resonances fall abruptly when substituting one Mn NN by Ga in the cluster, the one centered at 532 eV resulting absorbed by the following energy band. For two Ga atoms as NN none of the resonances shows up. Taking all this into account, it can be said that the average evolution of the theoretical spectra with Mn NN substitutions by Ga atoms nicely predicts the experimental results obtained for $LaMn_{1-x}Ga_xO_3$.

5. Discussion and conclusions

We have shown how electronic and structural degrees of freedom give rise to the pre-edge structures in the oxygen K-edge XANES spectra of two classical systems such as $LaFeO_3$ and $LaMnO_3$. All together, the systematic decrease of the pre-peaks with gallium dilution in the experimental spectra of $LaFe_{1-x}Ga_xO_3$ and $LaMn_{1-x}Ga_xO_3$ supported by the theoretical calculations, explains the origin of the pre-edge features as a mixing between 2p filled states of oxygen and 3d empty states of the transition metal. Although this interpretation was broadly accepted in the literature [8,10], the present experimental results conclusively confirm this conventional description.

Besides the evidence for the electronic nature of the pre-peaks, the MS calculations that we have performed, have enabled us to determine also their structural origin. It has been shown that the lower energy pre-peak is related to a 2p – 3d bond which is independent of the coordination geometry around the transition metal atom. For the formation of this state, only one O atom and one 3d-transition-metal atom in the cluster are needed. Furthermore, the polarization study carried out for $LaFeO_3$ with respect to the frame used in figure 6 in which the

bond direction is along y, has pointed out that the related O 2p – Fe 3d bond is of π symmetry (the same can be said for O 2p – Mn 3d bond in $LaMnO_3$). Therefore, to a first approximation this state comes from mixing of p_x and p_z oxygen orbitals with the d_{xy} and d_{yz} orbitals of the transition metal. It is to be noted that the 3d levels are still not split by the action of the crystal field since the transition metal is only bonded to one oxygen atom. As for the higher energy region in the pre-edge, it has been shown that the spectral features are related to the completion of the octahedral coordination geometry around the 3d-transition-metal NN atoms. Both their energy position and intensity are strongly dependent on the geometry around the absorber oxygen. From the polarized results obtained for $LaFeO_3$ it can be deduced that these resonances represent states of σ symmetry (again, the same can be said for $LaMnO_3$). Moreover, as their presence requires the completion of the oxygen octahedra (distorted or not) around the transition metal, i.e. when the degenerate 3d states are split in the t_{2g}-e_g symmetry bands; it follows that these resonances are due to hybridization of p_y oxygen orbitals with the local transition metal $d_{x^2-y^2}$ orbital, which belongs to the e_g manifold in octahedral crystal field. These states are very near the bottom of the band arising from the hybridization of the O 2p orbitals with those of the La 5d states (peak C in figures 2, 7, and 11) and can more easily form an extended band. Indeed they have been shown to be very sensitive to long-range order in the MS calculations within a large cluster of about 9 Å. This may explain why, in the experimental spectra, the pre-peak B is slightly more affected than the pre-peak A by Ga substitution: gallium doping progressively breaks the connectivity among transition metal atoms in the lattice.

Another significant result is the transfer of spectral weight from the pre-peaks (O 2p and transition metal 3d states mixing) to the following band in energy (O 2p and La 5d states mixing) upon Ga substitution. This finding seems to indicate that the oxygen charge tends to remain constant, in such a way that the 2p orbitals hybridize alternatively with same average weight with the accessible orbitals coming either from the transition metal atom or the rare earth one.

Summarizing, the joined experimental and theoretical study of the oxygen K-edge XANES spectra in the $LaB_{1-x}Ga_xO_3$ (B = Fe, Mn) series, has allowed us determining the characteristics of various relevant features in the spectra of the parent compounds $LaFeO_3$ and $LaMnO_3$. We have interpreted the states associated to the pre-edge structures and have found that they are highly sensitive to the type of bonding between oxygen and the 3d-transition-metal. As a final remark, we want to stress that the oxygen coordination geometry and especially the B-O distances, are fundamental factors for understanding the pre-edge energy region in the oxygen K-edge XANES spectra of transition metal oxides.

Acknowledgments

Financial support from the Spanish MICINN (project nº FIS2008-03951) and Diputación General de Aragón (DGA-CAMRADS) are gratefully acknowledged. The authors thank ELETTRA for granting beam time and the staff from the BEAR beamline for their kind assistance during the experiment. S. L. and V. C. thank DGA and MICINN, respectively for the research grants.

References

[1] Galasso F S 1990 *Perovskites and High Tc Superconductors* (New York, Gordon and Breach)

[2] Coey J M D, Viret M and Von Molnar S 1999 *Adv. Phys.* **48(2)** 167

[3] Khomskii D I 2006 *J. Magn. Magn. Mater.* **306** 1

[4] Müller J E, Jepsen O and Wilkins J W 1982 *Solid State Commun.* **42** 365

[5] Kohn W and Sham L J 1965 *Phys. Rev.* **140** 1133

[6] Natoli C R, Misemer D K, Doniach S and Kutzler F W 1980 *Phys. Rev. A* **22** 1104

[7] Rehr J J and Albers R C 1990 *Phys. Rev. B* **41** 8139

[8] de Groot F M F, Grioni M, Fuggle J C, Ghijsen J, Sawatzky G A and Petersen H 1989 *Phys. Rev. B* **40** 5715

[9] Abbate M *et al* 1993 *J. Electron Spectrosc. Relat. Phenom.* **62** 185

[10] Abbate M *et al* 1992 *Phys. Rev. B* **46** 4511

[11] Sarma D D, Rader O, Kachel T, Chainani A, Mathew M, Holldack K, Gudat W and Eberhardt W 1994 *Phys. Rev. B* **49** 14238

[12] Park J H, Chen C T, Cheong S-W, Bao W, Meigs G, Chakarian V and Idzerda Y U 1996 *Phys. Rev. Lett.* **76** 4215

[13] de Groot F M F, Faber J, Michiels J J M, Czyzyk M T, Abbate M and Fuggle J C 1993 *Phys. Rev. B* **48** 2074

[14] Sarma D D, Shanti N and Mahadevan P 1996 *Phys. Rev. B* **54** 1622

[15] Ravindran P, Kjekshus A, Fjellvag H, Delin A and Eriksson O 2002 *Phys. Rev. B* **65** 064445

[16] Komine S and Iguchi E 2007 *J. Phys. Chem. Solids* **68** 1504

[17] Blasco J, García J, Campo J, Sánchez M C and Subías G 2002 *Phys. Rev. B* **66** 174431

[18] Sánchez M C, García J, Subías G and Blasco J 2006 *Phys. Rev. B* **73** 094416

[19] Wu Z Y, Gota S, Jollet F, Pollak M, Gautier-Soyer M and Natoli C R 1997 *Phys. Rev. B* **55** 2570

[20] Wu Z Y, Ouvrard G, Gressier P and Natoli C R 1997 *Phys. Rev. B* **55** 10382

[21] Wu Z Y, Benfatto M, Pedio M, Cimino R, Mobilio S, Barman S R, Maiti K and Sarma D D 1997 *Phys. Rev. B* **56** 2228

[22] Nannarone S *et al* 2004 *AIP Conf. Proc.* **705** 450

[23] Joly Y 2001 *Phys. Rev. B* **63** 125120; revised version of July 2009

[23b] The explicit formula of the arctan is provided in the FDMNES reference manual: http:// www.neel.cnrs.fr/fdmnes/. We used default values for the maximum, centre and width of the arctangent, which are equal to 30, 30 and 15 eV, respectively.

[24] Taguchi H, Masunaga Y, Hirota K and Yamaguchi O 2005 *Mater. Res. Bull.* **40** 773

[25] Rodríguez-Carvajal J, Hennion M, Moussa F and Moudden A H 1998 *Phys. Rev. B* **57(6)** R3189

[26] Subías G, García J, Sánchez M C, Blasco J and Proietti M G 2002 *Surf. Rev. Lett.* **9(2)** 1071

[27] Yoshiya M, Tanaka I, Kaneko K and Adachi H 1999 *J. Phys.: Condens. Matter* **11** 3217

Figure captions

Figure 1. Normalized XANES spectra at the O K-edge of $LaFeO_3$ and $LaMnO_3$.

Figure 2. Normalized XANES spectra at the O K-edge of: (a) $LaFe_{1-x}Ga_xO_3$ (x = 0, 1/3, 0.5, 2/3, 0.8, 0.9) and (b) $LaMn_{1-x}Ga_xO_3$ (x = 0, 0.1, 0.2, 0.3, 0.5, 2/3, 0.8, 0.9).

Figure 3. Evolution of the A and B pre-peaks normalized integrated area in the spectra of $LaFe_{1-x}Ga_xO_3$ with Ga content (x).

Figure 4. MS theoretical absorption for the O K-edge of $LaFeO_3$ calculated for the O1 (4c site) atom within clusters of different radii: 2.0 Å (3 atoms), 3.2 Å (15 atoms), 3.5 Å (17 atoms), and 4.0 Å (19 atoms).

Figure 5. Picture of the cluster around the $O1_{abs}$ (4c site) up to 4.0 Å.

Figure 6. MS theoretical absorption for the O K-edge of $LaFeO_3$ calculated for the O1 (4c site) atom within a cluster of 4.0 Å for three different polarizations along the crystallographic frame: $\boldsymbol{E}\|[100]$, $\boldsymbol{E}\|[010]$, and $\boldsymbol{E}\|[001]$.

Figure 7. Comparison between the experimental XANES at the O K edge of $LaFeO_3$ and a converged MS theoretical calculation within a cluster of 9.1 Å (~ 260 atoms).

Figure 8. MS theoretical absorption for the O K-edge of $LaFeO_3$ calculated for the O1 (4c site) atom within a cluster of 4.0 Å as a function of the substitution of the two Fe NN by Ga atoms.

Figure 9. MS theoretical absorption for the O K-edge of $LaMnO_3$ calculated for the two oxygen atoms O1 (4c site) and O2 (8d site). For O1 (upper panel) within clusters of radii: 2.0 Å (3 atoms), 3.3 Å (15 atoms), 3.5 Å (17 atoms), and 4.0 Å (19 atoms); and for O2 (lower panel) within cluster of radii: 2.2 Å (3 atoms), 3.4 Å (17 atoms), 3.9 Å (18 atoms) and 4.4 Å (26 atoms).

Figure 10. Picture of the cluster around the $O2_{abs}$ (8d site) up to 4.4 Å.

Figure 11. Comparison between the experimental XANES at the O K-edge of $LaMnO_3$ and a converged MS theoretical calculation within a cluster of 9.1 Å (~ 250 atoms).

Figure 12. MS theoretical absorption for the O K-edge of $LaMnO_3$ calculated for the O1 (4c site) –upper panel– and O2 (8d site) –lower panel– atoms within clusters of 4.0 and 4.4 Å respectively, as a function of the two Mn NN substitution by Ga atoms.

Table 1. Radial distances distribution for the O1 (4c site) atom in $LaFeO_3$ up to 4 Å.

O1 (4c site)	
Atom	**Distance (Å)**
Fe (x 2)	1.9975
La	2.4580
La	2.5893
O2 (x 2)	2.8056
O2 (x 2)	2.8344
O2 (x 2)	2.8347
O2 (x 2)	2.8393
La	3.0294
La	3.1109
O1 (x 2)	3.4496
O1* (x 2)	3.9949

Table 2. Radial distances distribution for the O1 (4c site) and O2 (8d site) atoms in $LaMnO_3$ up to 4.0 and 4.4 Å respectively.

O1 (4c site)		**O2 (8d site)**			
Atom	**Distance (Å)**	**Atom**	**Distance (Å)**	**Atom**	**Distance (Å)**
Mn (x 2)	1.9683	Mn	1.9055	O2	3.2556
La	2.4217	Mn	2.1800	La	3.3830
La	2.5837	La	2.4453	O2	3.3959
O2 (x 2)	2.7315	La	2.6629	O2*	3.8110
O2 (x 2)	2.7476	La	2.7057	Mn	4.0192
O2 (x 2)	2.9116	O1	2.7315	O1	4.0896
O2 (x 2)	2.9625	O1	2.7476	Mn	4.1563
La	3.1550	O2 (x 2)	2.8863	Mn	4.1788
La	3.2364	O2 (x 2)	2.9045	Mn	4.1868
O1 (x 2)	3.4691	O1	2.9116	O2 (x 2)	4.3509
O1* (x 2)	3.9366	O1	2.9625	O2**	4.3601

Figure 1

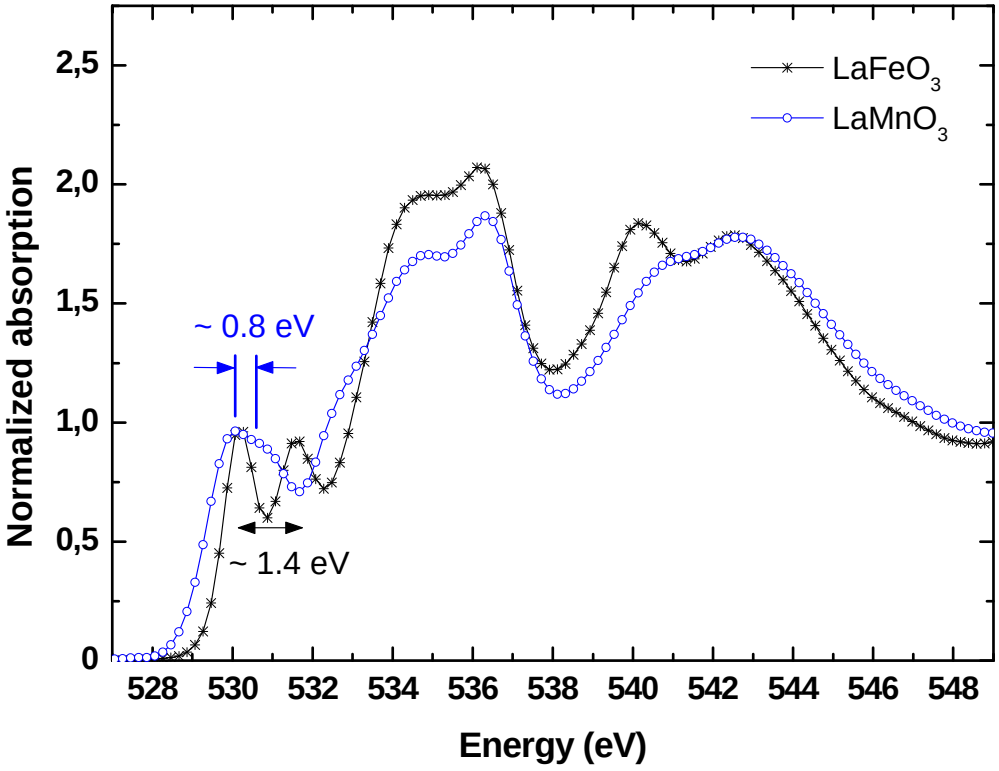
Normalized absorption
Energy (eV)
LaFeO3
LaMnO3
~ 0.8 eV
~ 1.4 eV
0
0,5
1,0
1,5
2,0
2,5
528
530
532
534
536
538
540
542
544
546
548

Figure 2

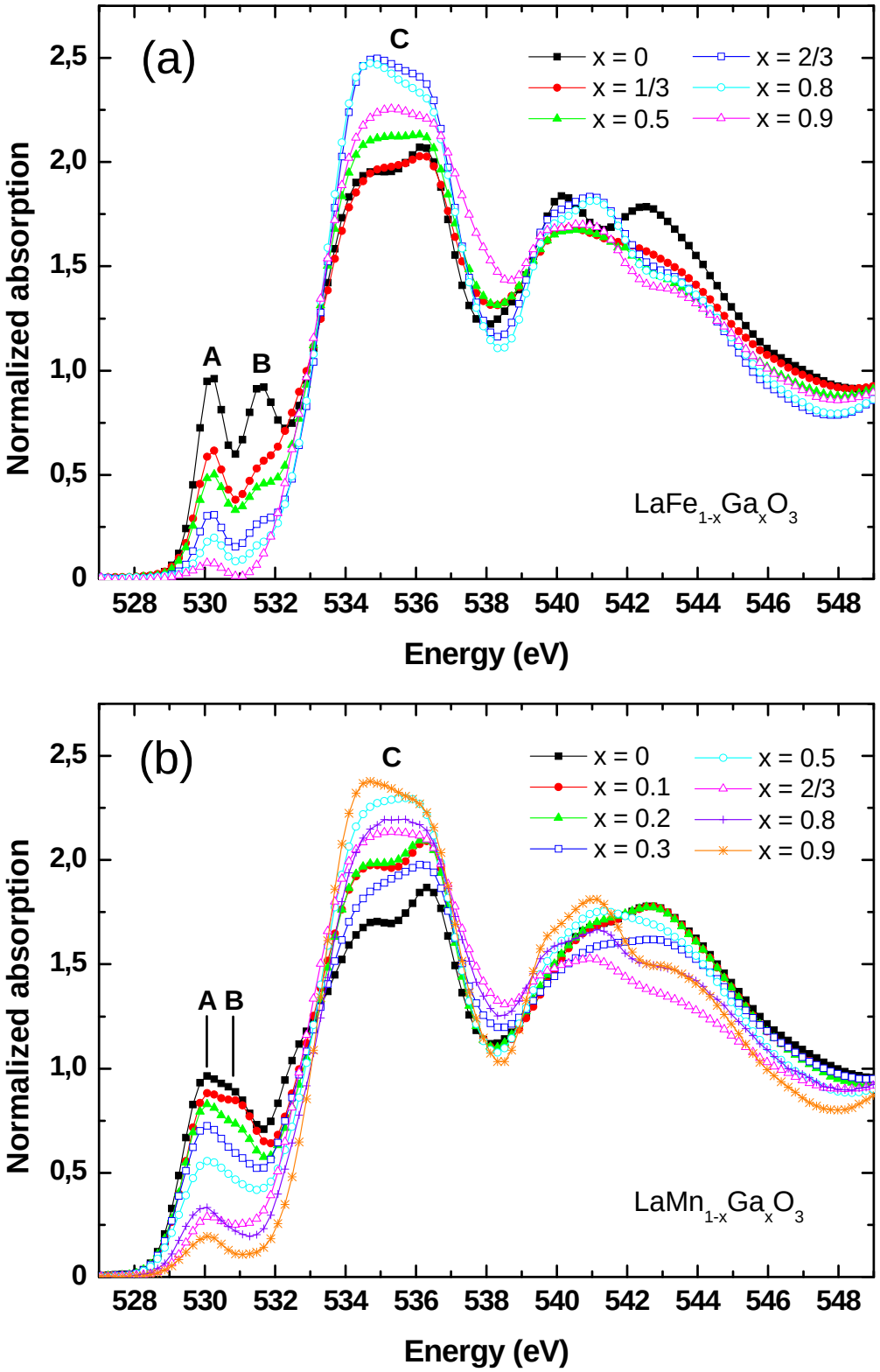
(a)
C
A
B
x = 0
x = 1/3
x = 0.5
x = 2/3
x = 0.8
x = 0.9
LaFe1-xGaxO3
Normalized absorption
Energy (eV)
(b)
C
A B
x = 0
x = 0.1
x = 0.2
x = 0.3
x = 0.5
x = 2/3
x = 0.8
x = 0.9
LaMn1-xGaxO3
Normalized absorption
Energy (eV)

Figure 3

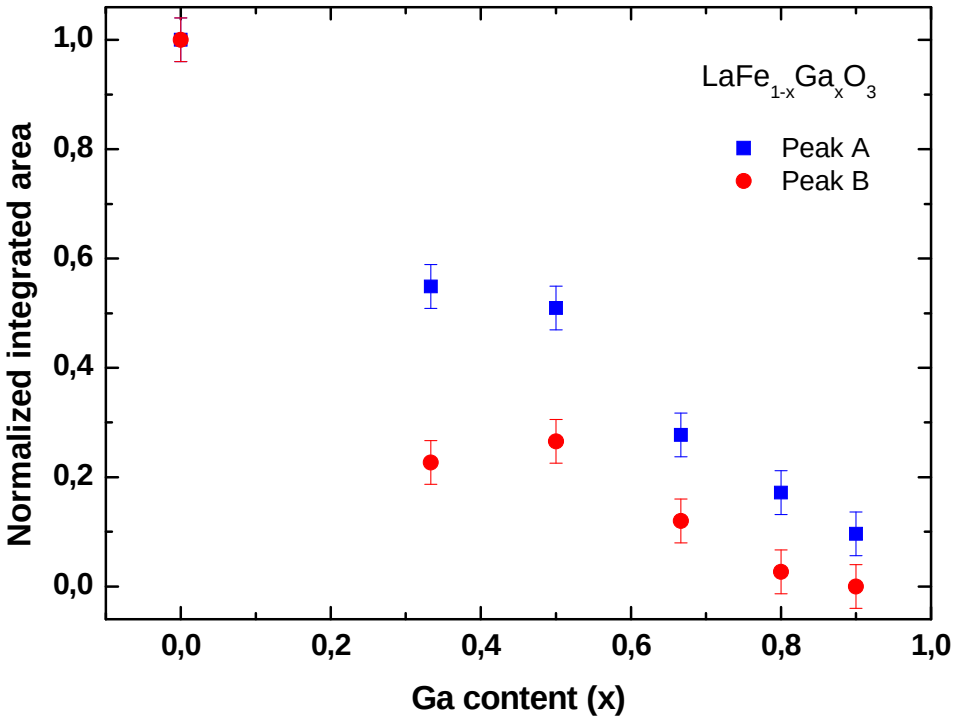
LaFe1-xGaxO3
Peak A
Peak B
Normalized integrated area
Ga content (x)
0,0
0,2
0,4
0,6
0,8
1,0

Figure 4

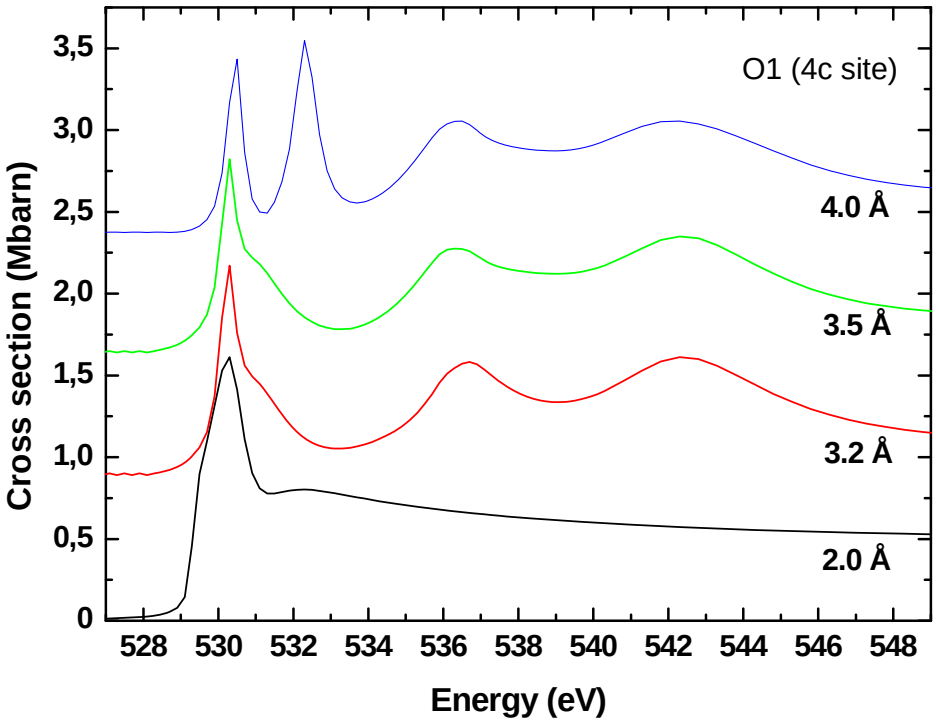
O1 (4c site)
4.0 Å
3.5 Å
3.2 Å
2.0 Å
Cross section (Mbarn)
Energy (eV)
0
0,5
1,0
1,5
2,0
2,5
3,0
3,5
528
530
532
534
536
538
540
542
544
546
548

Figure 5

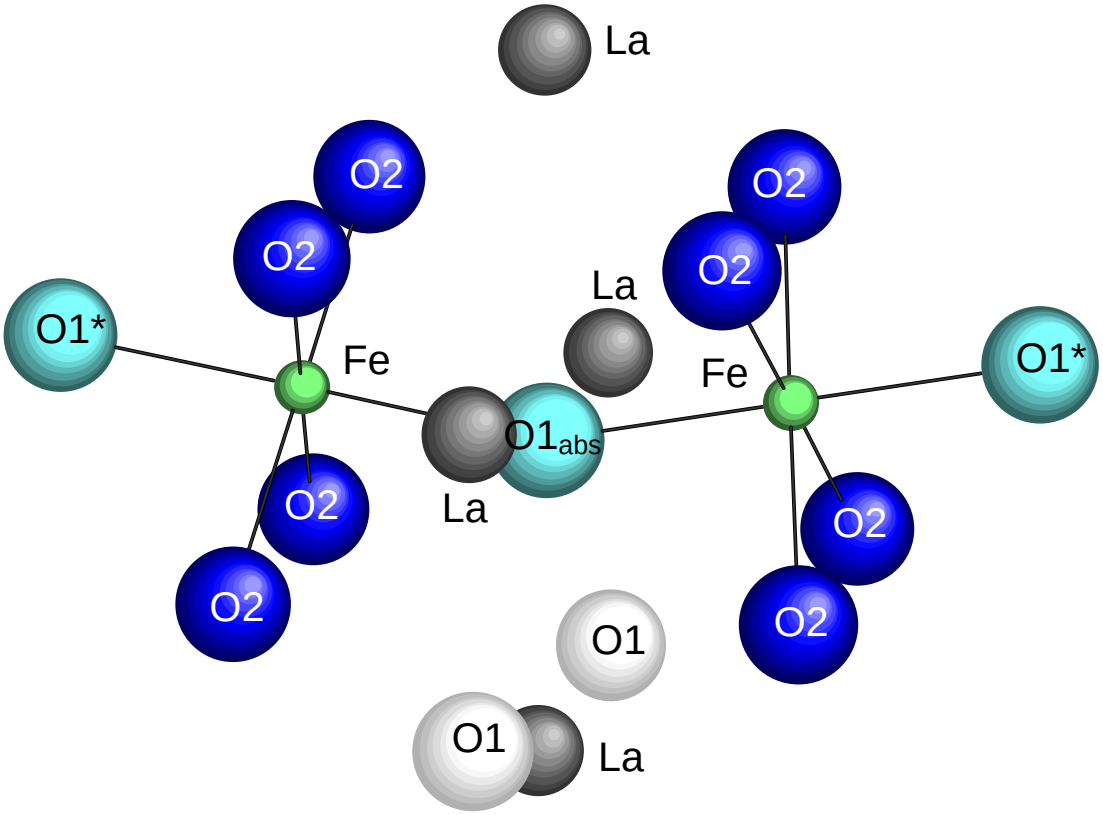

Figure 6

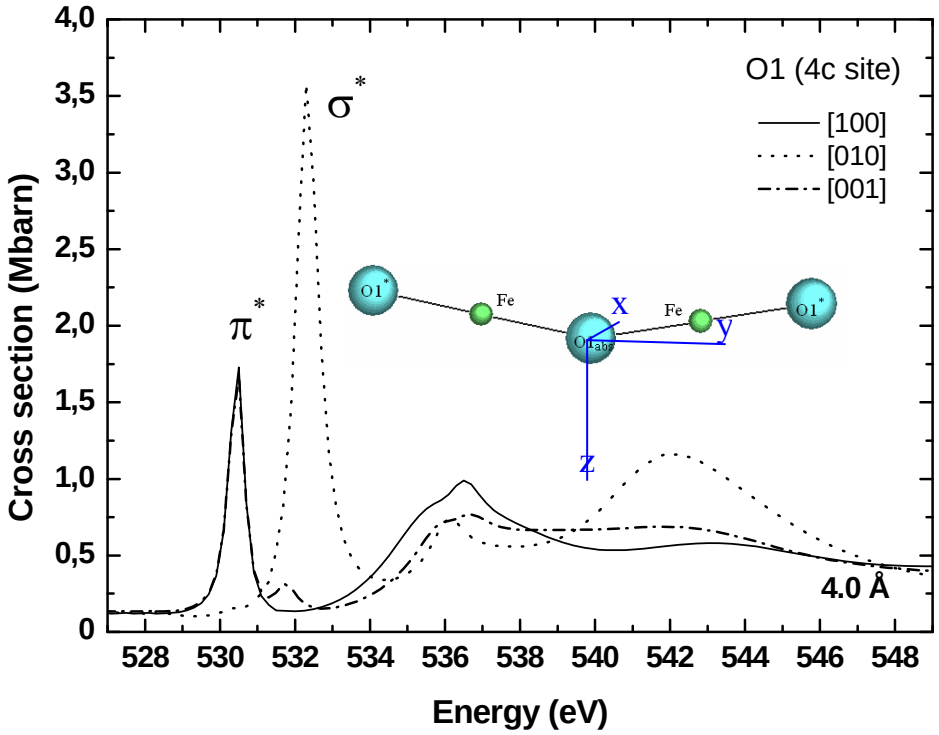
O1 (4c site)
[100]
[010]
[001]
σ*
π*
Fe
Fe
O1*
O1*
O1abs
x
y
z
4.0 Å
Cross section (Mbarn)
Energy (eV)
0
0,5
1,0
1,5
2,0
2,5
3,0
3,5
4,0
528
530
532
534
536
538
540
542
544
546
548

Figure 7

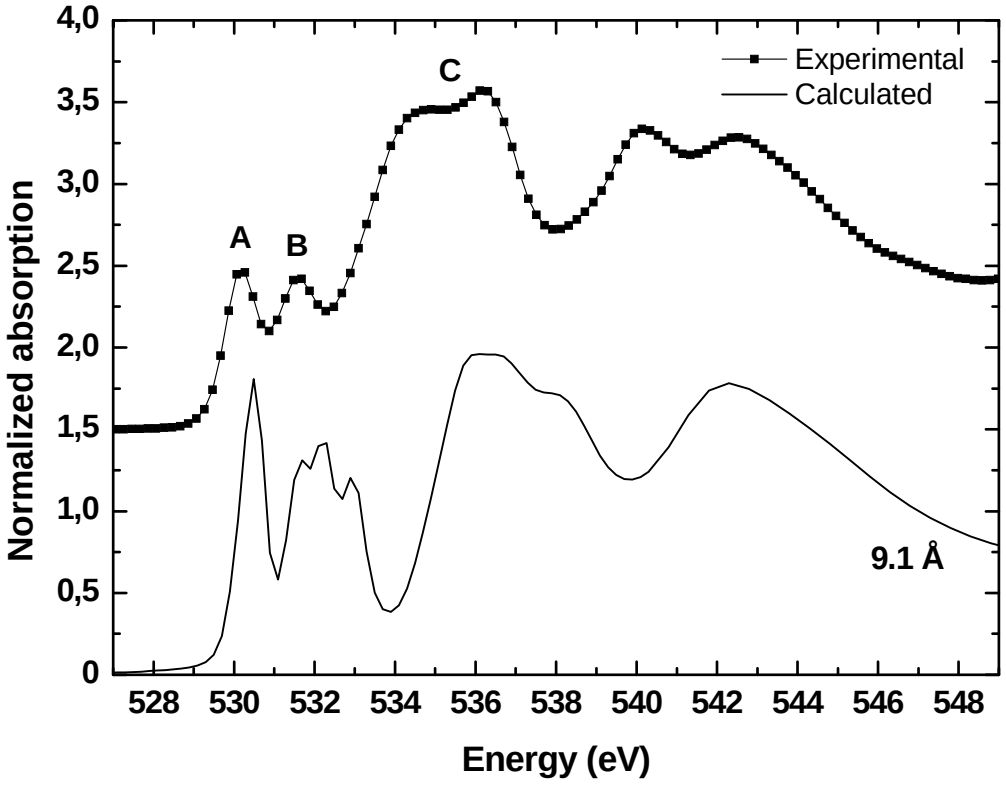
Experimental
Calculated
A
B
C
9.1 Å
Normalized absorption
Energy (eV)
0
0,5
1,0
1,5
2,0
2,5
3,0
3,5
4,0
528
530
532
534
536
538
540
542
544
546
548

Figure 8

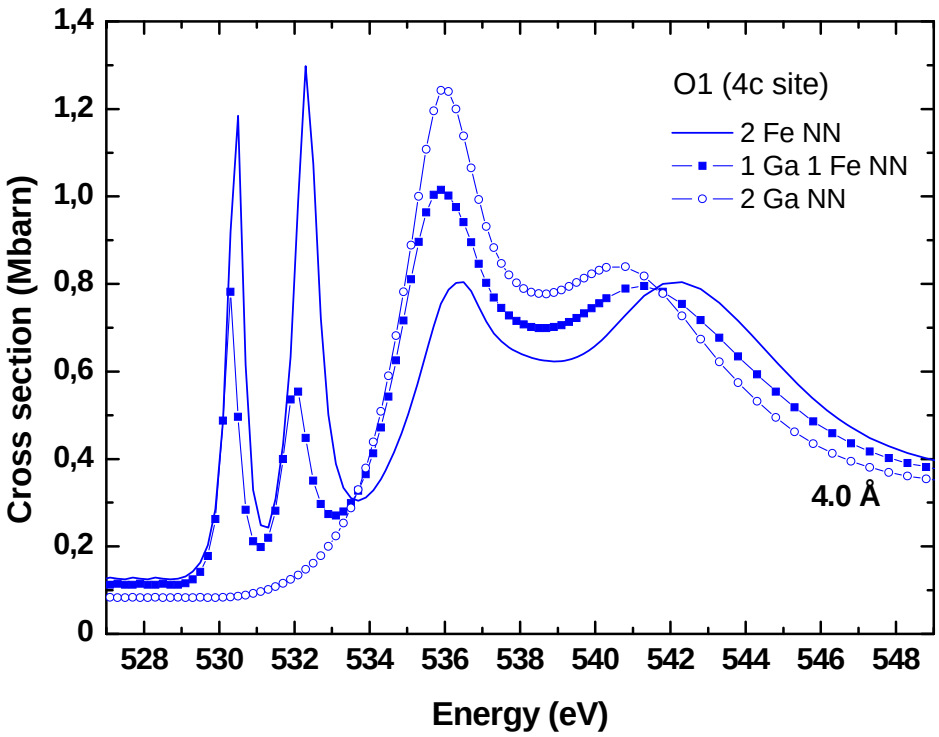
O1 (4c site)
2 Fe NN
1 Ga 1 Fe NN
2 Ga NN
4.0 Å
Cross section (Mbarn)
Energy (eV)
0
0,2
0,4
0,6
0,8
1,0
1,2
1,4
528
530
532
534
536
538
540
542
544
546
548

Figure 9

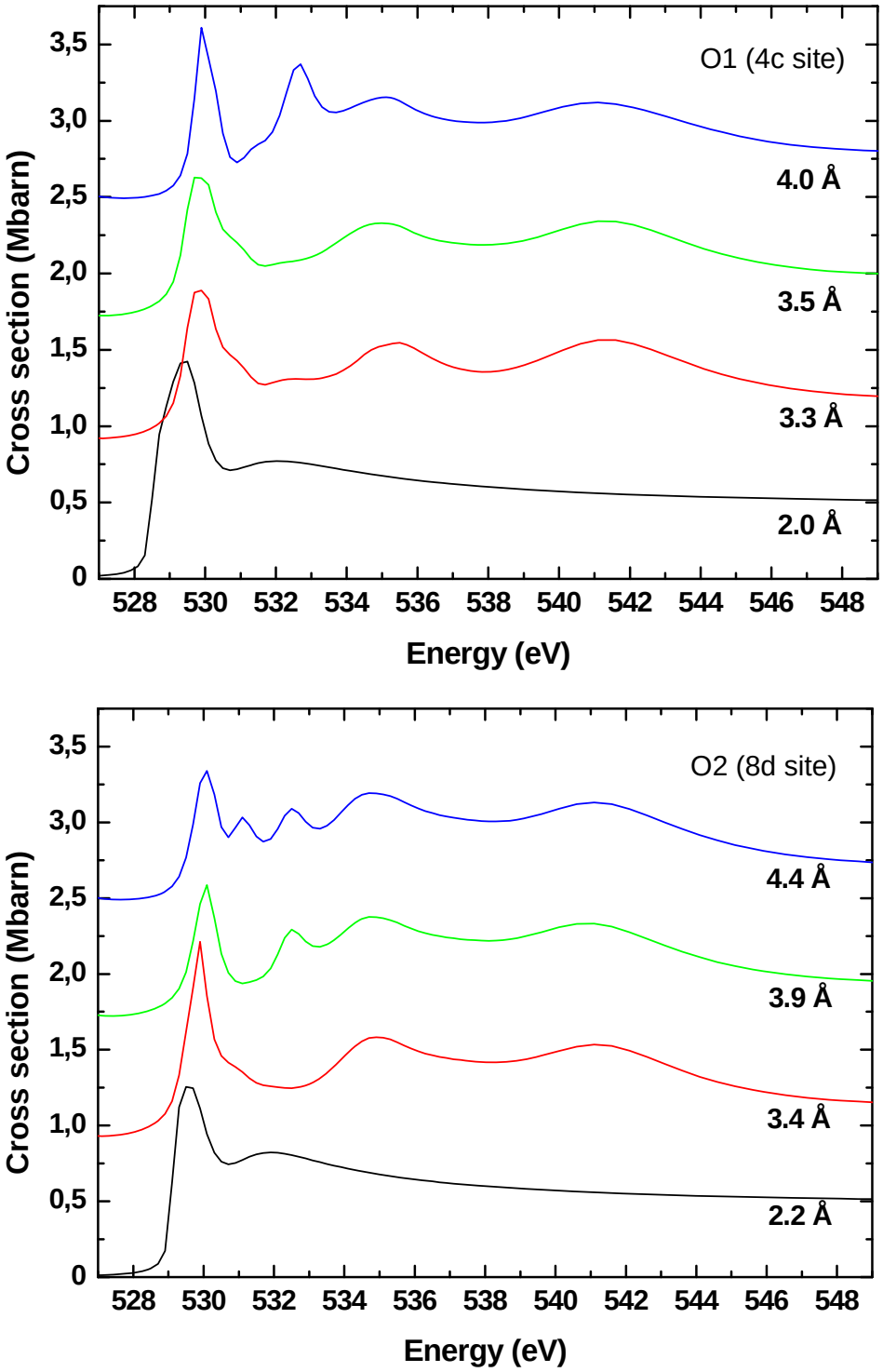
O1 (4c site)
4.0 Å
3.5 Å
3.3 Å
2.0 Å
Cross section (Mbarn)
Energy (eV)
O2 (8d site)
4.4 Å
3.9 Å
3.4 Å
2.2 Å
Cross section (Mbarn)
Energy (eV)

Figure 10

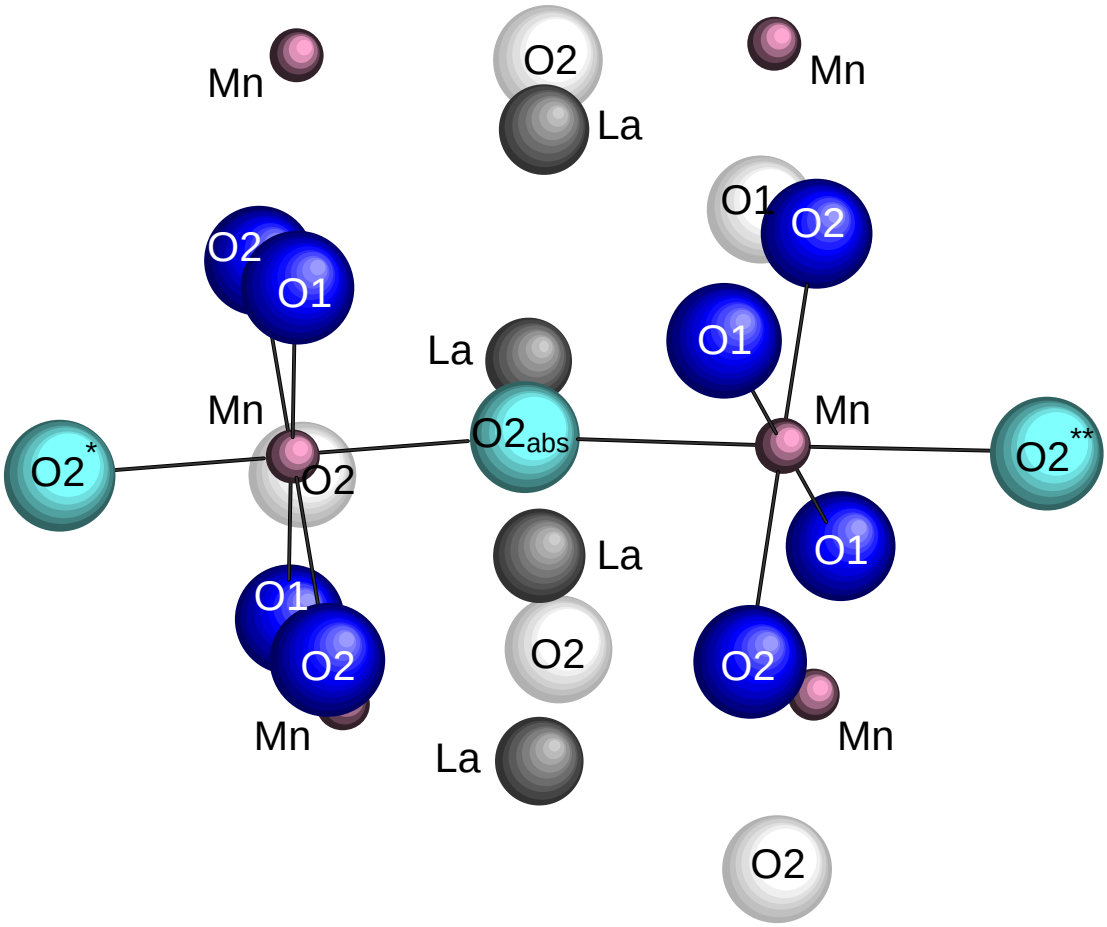
Mn
O2
La
Mn
O1
O2
O2
O1
La
O1
O2
Mn
O2*
O2
O2abs
Mn
O2**
La
O1
O1
O2
O2
O2
Mn
La
Mn
O2

Figure 11

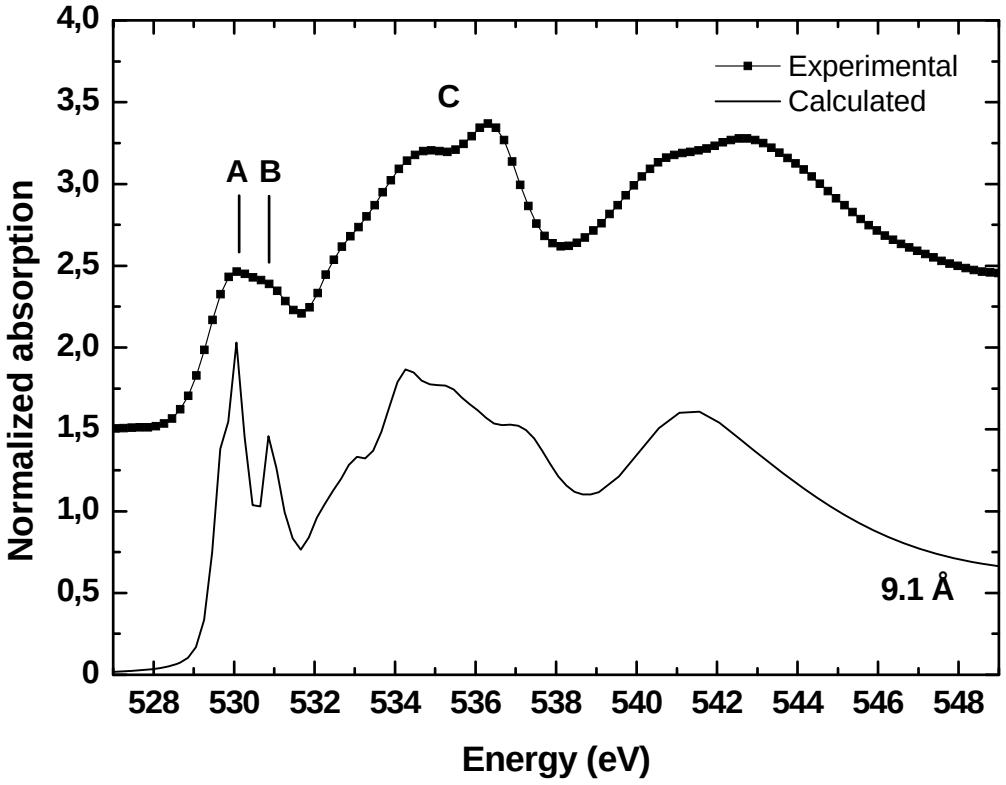
Experimental
Calculated
A
B
C
9.1 Å
Normalized absorption
Energy (eV)
4,0
3,5
3,0
2,5
2,0
1,5
1,0
0,5
0
528
530
532
534
536
538
540
542
544
546
548

Figure 12

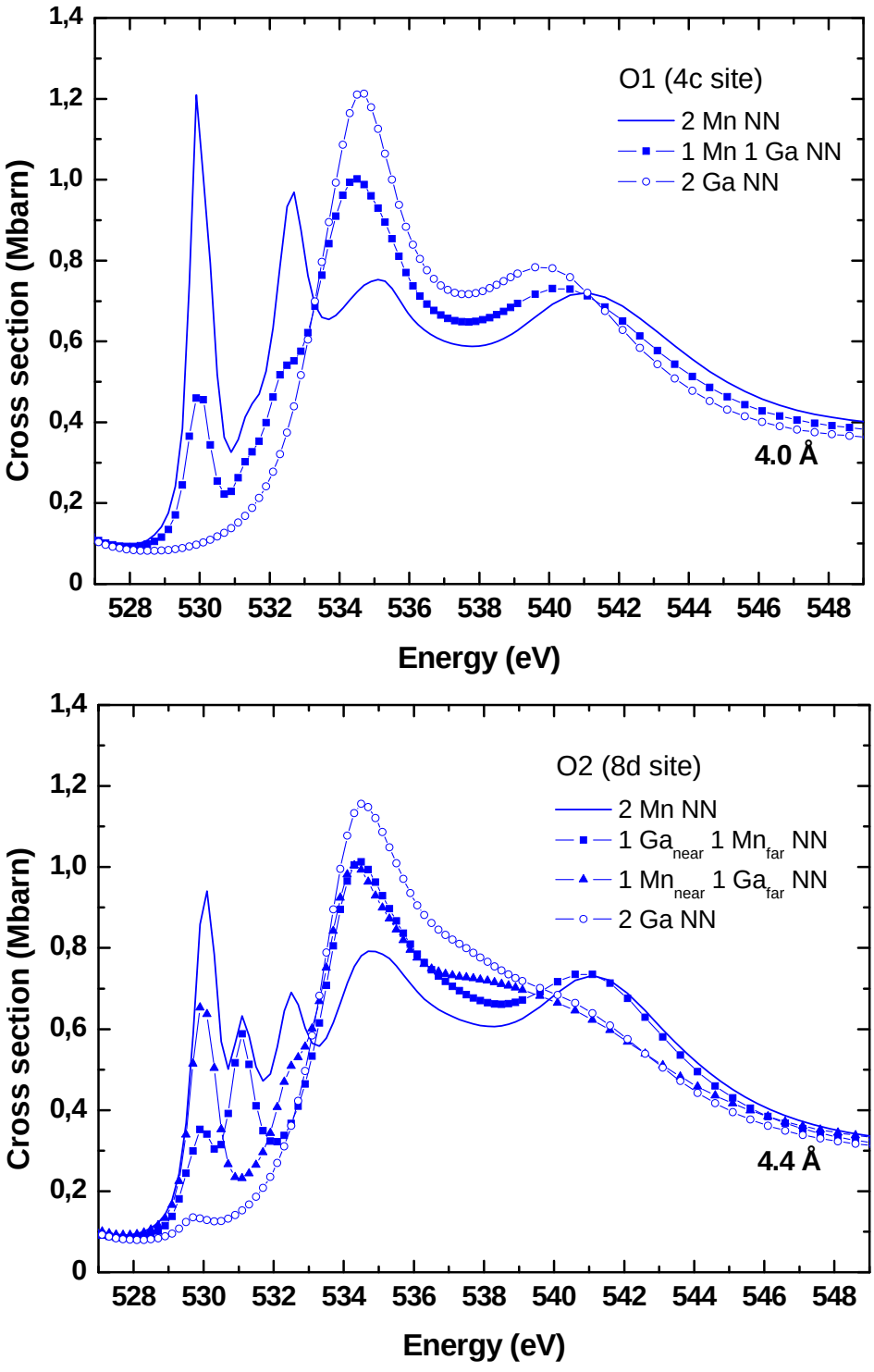
O1 (4c site)
2 Mn NN
1 Mn 1 Ga NN
2 Ga NN
4.0 Å
Cross section (Mbarn)
Energy (eV)
O2 (8d site)
2 Mn NN
1 Ga near 1 Mn far NN
1 Mn near 1 Ga far NN
2 Ga NN
4.4 Å
Cross section (Mbarn)
Energy (eV)